

# The Impacts of Morpho-Climatic Parameters on Pandemic Proliferations of Covid-19 between Expansion and Confinement in Semi-Arid Areas: Case of Batna City (Algeria)

DJAGHROURI Djamila<sup>1</sup>, ZERAIB Salah<sup>2</sup>, BOUDJELLAL Lazhar<sup>3</sup>, BENABBAS Moussadek<sup>4</sup>

<sup>1,4</sup> LACOMOFA Laboratory, University of Biskra

<sup>2</sup> University Batna 2

<sup>3</sup> Institute of Architecture and Urban Planning, University of Batna 1, ABE Laboratory, University of Constantine 3

## Abstract

The climate approach to urban planning related to urban pandemic mitigation strategies must be part of the sustainability agenda for the well-being and the health of the citizen. Although previous research has shown that the use of urban outdoor spaces enhances people's physical and mental health, lockdown policies around the world in the aftermath of COVID-19 have negatively impacted the well-being of communities and the sustainability of urban spaces. The interest of this paper is to verify if the urban morpho-climatic space conditions would influence its performance during covid-19 propagation. The work method adopted is based on investigation through bibliographical research on a great number of scientific journals' articles and international reports, while in the experimental part we used Envi-met software for numerical simulation for morpho-climatic environment.

The case study applies to two well-chosen urban spaces, in Batna city (Algeria), which differ in morphology and density, as well as, in the spread of Covid-19 virus between them. The results of our summer 2020 conducted work revealed morpho-climatic parameters that affect the behavior of epidemics in urban areas, which allowed us to highlight the optimal performance of such urban space to be retained to mitigate the spread of the virus.

**Key words:** public space; micro-climatic performance; urban morphology; covid-19; numerical simulation; city of Batna.

## INTRODUCTION

Since ancient times, humanity has suffered from devastating epidemics in which quarantine was considered the main means to limit the spread of viruses between people. Historically, we note that architecture and town planning have had an important and fundamental role in moderating deadly health crises. Particularly with the emergence of the hygiene movement, that has contributed mainly to preserving large cities from the contagion of epidemics [1] Haussmannization of Paris of Paris as an example, and the impact of the modern movement and its principles in terms of architecture and town planning on the health of populations, which came in response to the great epidemics of the 19th and 20th centuries.

Pandemic moderation strategies should be part of the sustainability agenda, supporting the third Sustainable Development Goal, relating to the well-being and good health of citizens [2]. The major problem facing cities is the high population density, which allows the spread of infectious diseases [3]. In this context, the corona virus pandemic is causing a state of emergency around the world, forcing governments to take restrictive measures; Confinement and social distancing are the two recommended solutions. The global strategy to combat Covid-19 to slow its transmission and reduce the mortality associated with covid-19, advocates, through the World Health Organization, physical distancing measures at the population level, including self-isolation [4].

Faced with this delicate provision, international health systems have applied non-curative preventive practices like full and partial confinement in order to mitigate the impact of COVID-19 on peoples [5]. What follows is based on content from high-impacted scientific journals on the nature of urban spaces, epidemiology, virology, environmental science, public health, and urban systems related to immunity.

Urban space design is a means of influence for planning healthy cities, urging physical and mental health benefits [6], nevertheless, spatial containment actions must avoid provocative factors ; such as extreme densities, over-connected street networks, monofunctional neighborhoods, insufficient natural ventilation, lack of sunshine. All of which increases the risk of epidemics [7] , however, urban spaces could maintain isolated physical and psychological restorative environments [2] .

In this context, spatial distancing, of at least 1m with others, while preserving social ties is more appropriate and could reshape the urban space in order to make our cities healthier while limiting the spread of the pandemic [4,8–10] . Recent studies on infectious disease control have highlighted climatic influences on disease containment and spread. The results led to predictive models of viral infections based on micro-climatic parameters [10] .

The estimation of micro-climatic conditions in outdoor urban spaces requires a thorough knowledge of many parameters related to the urban environment, such as air temperature, relative humidity, air speed, rainfall, and above all; solar radiation and ventilation

In this regard, from the review of the literature, some previous research has proven the correlation of micro-climatic conditions with respiratory diseases [11] , and that there is an association between the accelerated spread of COVID-19 virus and prevailing air speed [12,13] . In 2020, Stevens and Tavares proved that cities with well-ventilated urban spaces reduce contagious respiratory diseases and generate resilient urban environments [5,14]. Furthermore, social distancing and ventilation are applied to control the COVID-19 pandemic. The study indicated that 1.6 to 3.0 m (5.2 to 9.8 ft) is the safe social distance when considering aerosol transmission of large expired droplets during dialogues, while the distance can be up to 8.2 m (26 ft) if we consider all droplets in a still air environment [15] .

Although minimum ventilation or fresh air requirements should vary depending on remoteness conditions, length of exposure and efficiency of air distribution systems, effective natural ventilation is an influential factor in reducing the risk of contagious infections. Recent research has ruled the accelerated spread of the COVID-19 virus relative to the prevailing wind speed [10,13] . Nevertheless, precautions should be observed in terms of increasing ventilation rates, as staying in the same direction of airflow with an infected person would increase cross-infection rates [10] .

As for solar radiation, solar ultraviolet radiation proves to be the most influential on public health [16] , it suppresses adaptive immunity while stimulating non-specific innate immunity. Consequently, it acts on the reduction of mortality possibilities [17] .

That is why doctors recommend daily sun exposure from 10 a.m. to 3 p.m. only for 15 to 30 minutes, depending on skin color. The researchers also added that the recommended daily amount for infants 0-12 months is 400 international units (IU), while that for people 1-70 years old is 600 IU. However, the recommended daily exposure amount increases to 800 (IU) for people over the age of 70 [18,19] . Likewise, the preservation of good air quality contributes to the photosynthesis of vitamin D. In this regard, air pollution is one of the main factors leading to its deficiency in most urban settings. By blocking the ultraviolet rays responsible for the process of photosynthesis [20] . Temperature and relative humidity are additional factors that affect the microclimate of urban spaces and affect the occurrence of respiratory diseases. Franch-Pardo asserted the relationship between mortality rates in Wuhan (the epicenter of the COVID-19 virus) and both temperature and relative humidity ranges (Franch-Pardo et al. 2020). Wang supported Lowen's findings, stating that high temperature and high humidity, respectively, reduce COVID-19 transmission [21] .

Our observation stipulates that the Covid-19 pandemic is dependent on the major cities of developed countries. Very little research has been undertaken in Third World cities, particularly in Algerian cities, which have experienced significant spread of Covid-19. This is the case of Batna city, which we have chosen, to highlight the influence of environmental spatial parameters on the contagion of epidemics in general and the Covid-19 pandemic in particular.

To wonder to what extent urban environments would reduce the spread of the virus; this article takes up two urban scenarios to highlight the correlation between the spread of epidemics and the environmental spatial parameters, between the planned individual (subdivisions) and collective housing, respectively with a high rate of spread of the virus and a weak diffusion for the latter. (Health department Data of Batna city, 2020). Our research is based on in situ measurements, modeling and simulation to calculate the micro-climatic parameters of the two urban sites (air temperature, relative humidity, speed air, solar radiation, etc.). Also emphasizes the impact of other environmental

factors, including air quality, in addition to spatial factors regarding the dimensions of space and the spatial distance required to reduce the spread of the virus. Based on the literature review, sufficient exposure to sunlight and natural ventilation affect the spread of the pandemic. Nevertheless, the study aims to synthesize the dense findings of the literature review through a quantitative assessment framework. It highlights the main parameters influencing pandemic mitigation in urban areas, namely: Spatial parameters and micro-climatic evaluation. Table 1.

**Table 1.** Representing the quantitative assessment framework of morpho-climatic parameters required for pandemic mitigation of urban spaces

	<b>Morphological parameters</b>		
parameters	Scale	Impact	Reference
Space dimensions (H:W ratio)	- 1:2 or max. 1.5:2, of 12 m to 24 m - side length average 0.5–0.75	- Enable solar exposure - Enable psychological relief - Enable adequate air ventilation.	[31, 32]
Estimated number of users (1.80 m apart)	1.1-2 m apart	-Reduce rates of cross- infection.	[11, 33–35]
	<b>Climatic parameters</b>		
Daily exposure to solar radiation (kwh/m <sup>2</sup> )	-Low < 4,5 KWh/ m <sup>2</sup> -Moderate 4,5–5,5 KWh/m <sup>2</sup> -High >5,5 KWh/ m <sup>2</sup>	- High solar radiation cause skin burn and would lead to skin cancer.	[16,17,20,27–30]
Natural ventilation – air speed (m/s)	- <2.5 m/s - 2.5–5 m/s - >5 m/s	- Dilute infectious droplets - Enable droplets dispersion and avoid their accumulation. - Decrease infection Improve mental health	[5,12,14,25,31–33]
Air temperature (°C)		- High temperatures decrease the spread of the virus than low ones.	[12,21,34,35]
Relative humidity%	-Low <50% -Suitable: 50–70% - High >70%	- Higher relative humidity % decreases - The spread of the virus than low percentages.	[12,34–36]
	<b>Air quality index (AQI)</b>		
Air quality index (AQI)	- Healthy <50 % - Moderate 50 <and <100 - Unhealthy >100	- Decrease azmatic complications. - Decrease chest infection - Help in recovery phases	[10,20]

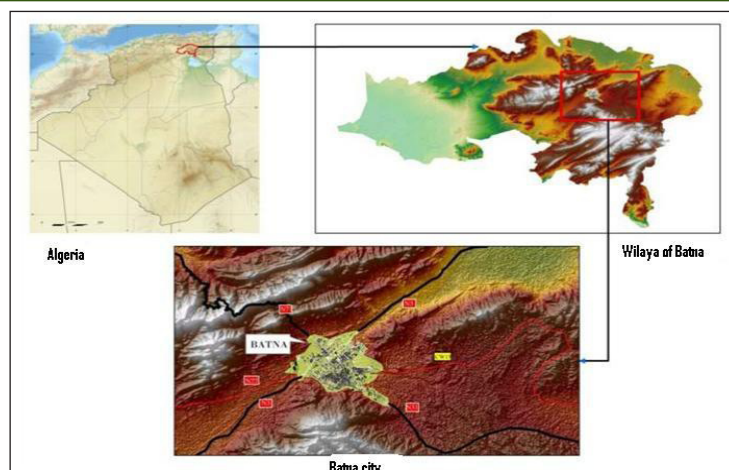
This estimate has prioritized and categorized spaces with compliant micro-climatic behavior so that they engage in public life during periods of confinement. [11, 33–35]

### Geographical and Climatic Context of Batna City

This study is on the city of Batna, an area in the eastern part of Algeria, located between 06° and 17° East longitude, and between 33° and 56° North latitude, at an altitude of 1058 m above sea level. The territory of the city of Batna is almost entirely part of the physical ensemble formed by the junction of two Atlases (Tellian and Saharan). Figure1.

This position gives it a semi-arid climate, characterized by a hot and dry summer with maximum temperatures reaching 36.4°C in July, and a cold and humid winter, with minimum temperatures reaching 0.4°C in January (Period 2011-2020 provided by the meteorological station of Batna).

According to real-time satellite data and air quality indices, the city of Batna unveiled a moderate air pollution level of 57 US AQI, the dominant pollutant is (PM<sub>2.5</sub>) with a concentration of 18, 1 µg/m<sup>3</sup> (standard established by the EPA Environmental Protection Agency. Main pollutant: Fine particles (PM<sub>2.5</sub>).

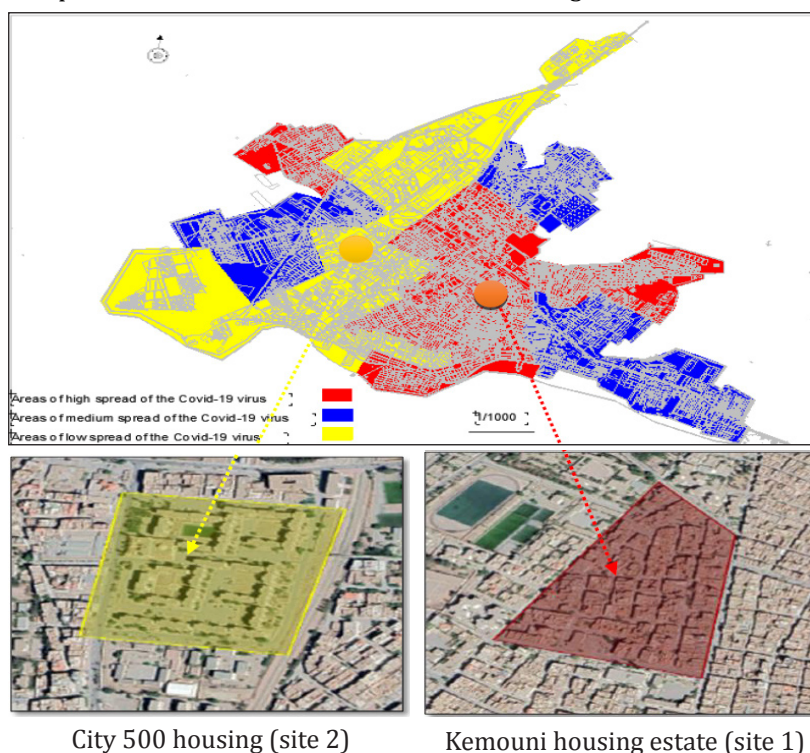


**Figure 1.** Location of Batna city.

### **Presentation of the Case Study: The Investigation Site**

Our study concerns two well-chosen urban fabrics in the city. These two urban fabrics represent a clear distinction in the spread of Covid-19 relating to their morphological distinctions and urban density, to which we will return later. The two fabrics represent regulated urban forms in two housing typologies namely; collective housing, and individual housing (These two urban fabrics are found on either side of Biskra road axis, in the ZHUN of Batna city's East extension. The first, parceling Kemouni, referred here as the site (1), is a district built in the 1970s (Older), the second is a collective housing district of 500 housing units, built between 1974 and 1984 as part of the ZHUNs in Algeria, named by the site (2). The choice of these two sites was made according to three criteria:

- a- Urban density, where the site (1) is very dense, while the site (2) is looser,
- b- The morphological indicators at the level of the exterior spaces, which are; the ratio (H/L) and the sky view factor (SVF).
- c- The big difference in the spread of the Covid-19 virus between them. Figure 2.



**Figure 2.** Location of the study area and distribution of the spread of Covid-19 in the urban sectors of Batna city







Although these sites are located in the busiest part of the city, they have been severely affected by the lockdown following the spread of the COVID-19 virus.

This is confirmed by statistics from the Batna health department, which indicates that the rate of cross-infection with Covid 19 in site (1) is high, up to 55%, and it is more important than the site (2), where the rate is lower up to 15%.

The distribution of the spread of Covid-19 in the urban sectors of the city of Batna according to the statistical data of the health directorate of Batna Wilaya, 2020, justifies our choice, where the distribution of Covid-19 between them is very distinct according to their morphological distinctions and both urban and population densities. Table 2.

**Table 2.** Characteristics of the two study sites.

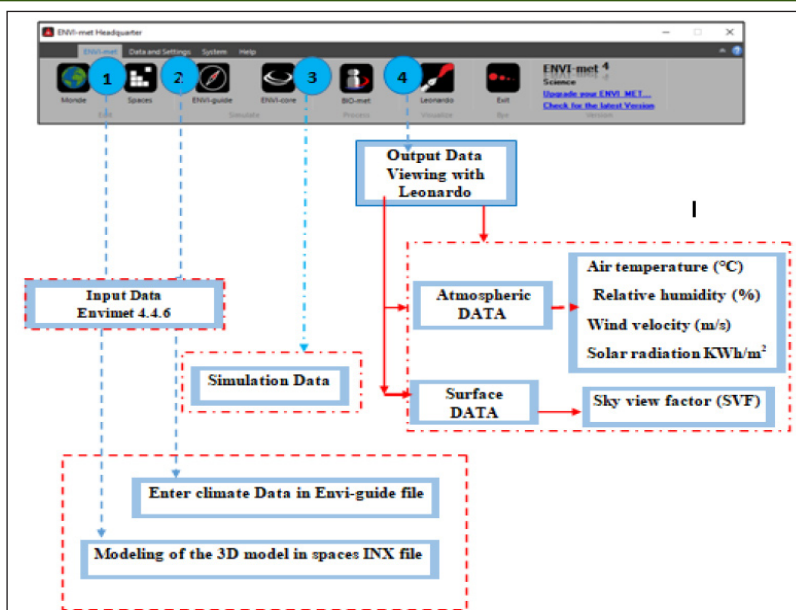
Study sites	Site Features
 <p>Kemouni housing estate : site (1)</p>	<p>Type: First self-built housing estate  Year built: 1970  Area: 120360 m<sup>2</sup>  Number of plots: (326 plots)  Built surface: 96296.00 m<sup>2</sup> _  Unbuilt area: 24064.00 m<sup>2</sup>  Height of constructions: R+1 up to R+4  Urban density ( CES) : 67%  Population : 2608 inhabitants  Urban area to strong spread of the Covid-19 virus</p> 
 <p>City 500 housing : site (2)</p>	<p>Type: collective housing  Year built: 1974-1984  Area: 65824 m<sup>2</sup>  Built area: 11190.08 m<sup>2</sup>  Unbuilt surface: 54633.92 m<sup>2</sup>  Building height: R+5  CES urban density: 17 %  Population: 2500 inhabitants  Urban area to low spread of the Covid-19 virus</p> 

## WORKING METHOD

Beside a dense bibliographic research applied in this context, we used an investigative approach based on the method of quantitative assessment of the spatial and environmental parameters necessary to mitigate the pandemic of urban spaces. The experimental concerns; in situ measurements in the first place, and in the second place; modeling and simulation using the software Envi-met pro version 4.4.6 [37]. Which deals with the effects of microclimatic conditions, the dimensions of the space, and in addition to the number of users of the spaces to be determined, we can deduce the spatial performance of the local climate on the spread of epidemics in the regions of the urban area. In line with the objectives of this research, we generated parametric measurements and numerical simulations using the professional version ENV-met 4.4.6 at both sites.

This allowed us to calculate the values of air temperature (°C), relative humidity (%), solar radiation (KWh/m<sup>2</sup>) and air speed (m/s), in order to reach the local climate performance of the two urban spaces, during the pandemic. According to a review of the literature, solar radiation and natural ventilation are major climatic factors affecting the risks of infection due to the spread of the COVID-19 virus. In this respect, numerical measurements are viable tools to calculate these parameters [37].

From the comparison between the two sites in terms of their spatial and environmental parameters, we can deduce, within them, the behavior of the COVID-19 epidemic, during the summer of 2020, according to the processes below. Figure 3.



**Figure 3.** Diagram showing the working process

## Numerical Simulation

ENVI-met is a three-dimensional prognostic climate model, which calculates the dynamics of the microclimate using fundamental physics based on the principles of fluid mechanics, thermodynamics and the laws of atmospheric physics. In particular, it allows the simulation of microclimatic interaction between urban surface, vegetation and atmosphere, and the analysis of the fine-scale effects of urban design in a microclimate under different meso-scale conditions [37].

ENVI-met has been widely used due to its ability to combine and consider spatial variations of the four meteorological variables influencing thermal comfort. According to research [38–40]. The results of ENVI-met software are more accurate and reliable in comparison with other software. The two scenarios, respectively, of the site (1) and (2), represent a variation in the urban morphology; each of them has a regulated urban form in two housing typologies, namely individual housing, for the site (1) and the collective, for the site (2).

## Simulation Method

To simulate the selected corpus, we took the two sites, corresponding to the horizontal microclimate scale. Both sites are modeled by ENVI-met pro version 4.4.6 using an orthogonal geometric grid whose spacing for directions (x, y) is (2 m, 2 m), and z is 20 m, summarized according to Table 3.

The modeling reproduces the 3D buildings, the ground, and the vegetation. The floor and wall materials of each fabric are identical in both cases.

**Table 3.** Data from the digital models of the two-site. Scenarios (1) and (2) modeling by ENVI-met pro version 4.4.6.

Model dimensions	First sample site (1) Kemouni district	Second sample site (2) 500 housing district
Horizontal grid study area	220m x 200m	120m x 140m
Horizontal resolution	$\Delta x = 2\text{ m}$ $\Delta y = 2\text{ m}$	$\Delta x = 2\text{ m}$ $\Delta y = 2\text{ m}$
Vertical grid study area	20m	20m
Vertical resolution	$\Delta z = 2\text{ m}$	$\Delta z = 2\text{ m}$


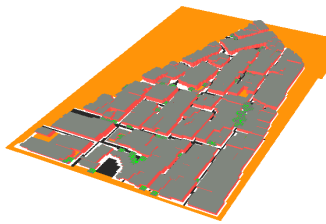

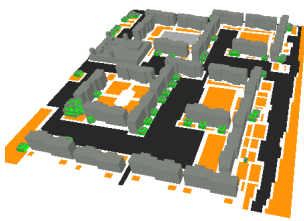
The simulated time interval extends from 8:00 a.m. to 4:00 p.m. along July 26, 2020, considered the hottest day, according to the climatic parameters for the month of July. It is also the day, when people visit the site extensively, while on that day, isolation was from 5 p.m. to 7 a.m. This choice is considered as the most unfavorable case of the summer period for this semi-arid climate where the meteorological data is introduced into the ENVI-met configuration file according to table 4

**Table 4.** Input configuration data applied in the ENVI-met simulations. The main parameters introduced to the \*.cf file. Simulation input data (inputs).

<b>Situation of the two sites</b>	Batna, Algeria Longitude 6.17 E Latitude: 33.56 N Altitude: 1058m North=45
Type of climate	Climate: semi-arid and dry climate in summer
simulation day	Typical hot summer day, 26.07.2020
Simulation time	From 07.00 a.m. to 6.00 p.m.: (12 hours)
<b>Climatic parameters:</b>	
Average wind speed (m/s)	2.50m/s
Wind direction	180.00 north
Average relative humidity (%)	28%
Average temperature (°C)	31°C
<b>Urban data</b>	
Urban density site (1)	67%
Urban density site (2)	17%
<b>Buildings:</b>	
Average height of the site section (01)	09m
Average height of the site section (02)	15m

In the ENVI-met, a visualization tool (LEONARDO) makes it possible to visualize the results of the modeling, in two dimensions 2D as in 3D (three dimensions). As a result, numerical models for different simulation scenarios of the two urban sites were designed, according to table 5.

**Table 5.** Modeling of the scenarios of the two sites n° (1) and (2) “2D model area and 3D model area created using ENVI met, showing the exterior spaces and the buildings.

Scenarios	2D model area	3D model area
Scenario site (1)	 <p>Urban density: 67% very dense fabric</p>	
Site Scenario (2)	 <p>Urban density: 17% loose fabric</p>	

## RESULTS AND DISCUSSIONS

After studying, the two main open spaces of the habitable urban fabrics in Batna, through the spatial factors concerning the dimensions of the space and the spatial distance required to reduce the spread of the disease. The evaluation prioritized and categorized spaces with adequate microclimatic behaviour to be engaged in public life during lockdown periods, according to table 01.

### The Evolution of the Morpho-Climatic Parameters Impact on the Spread of the Pandemic in the Two Urban Configurations

It presents the impact of these parameters on pandemic mitigation plans, illustrates related references, and refers to the parameters identified in the literature review. On the one hand, it identifies the spatial characteristics of urban space. It includes the aspect ratio (H/W) and the estimated number of users using the spatial distance from 1.80 to 2 m apart. At the same time, it highlights the climatic parameters that affect public health.

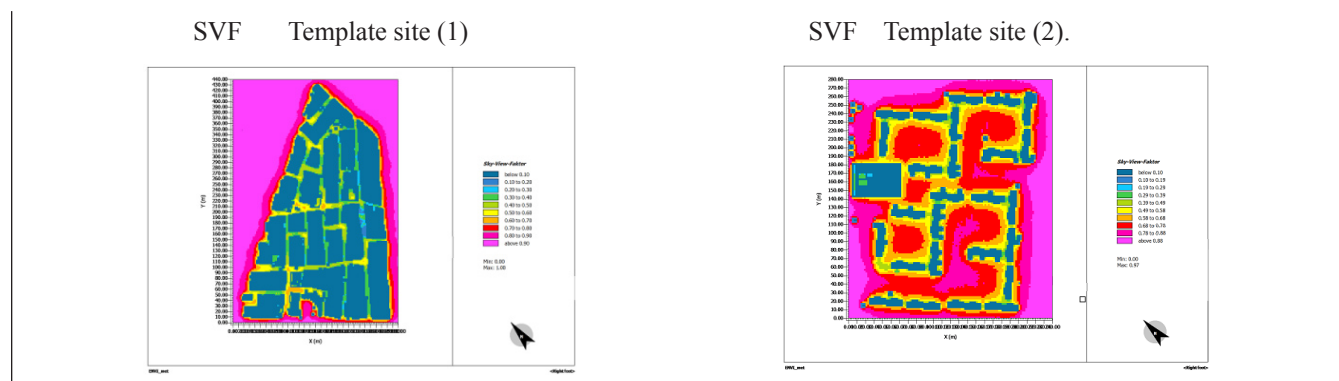
### Comparison between the Morphological Parameter Effects on the Pandemic Spread in the Two Urban Configurations

According to [41] the morphological indicators at the level of outdoor spaces are; the ratio (H/L), sky view factor (SVF), and orientation, which in our case, for both sites is (North - East)).

We define the sky view factor as the solid angle under which we can see the sky from an urban space. Its value varies from (0 to 1), 1; when the sky view is free of any obstructions, down to 0 where the view of the sky is totally obstructed. It corresponds to the portion of sky observed from the surface considered [42] .

The ENVI-met model makes it possible to calculate the sky view factor; the calculation takes into account the spatial characteristics of the urban fabrics and their immediate environment. The average sky view factor is very distinct between the two urban configurations. Figure 4.

Figure 4. Spatial distribution maps of the SVF deviation: the site (1) model on the left, the site (2) model on the right.



Based on the SVF spatial distribution map between site model no. (1) and site model no. (2). It illustrates high values of SVF in red color, equal at (0.80) in site no. (2), where the H/L ratio= 0.27 and the density is around 17%, while the lower values (equal to 0.40), are represented in green color in site no. (1), where the H/L ratio=1.15 and the density is estimated at 67%. These values are in the 500 dwellings' city where the spacing between the buildings are large and relatively constant over a long distance (56m), which makes their geometry open to the sky. (Average value of SVF= 0.80).

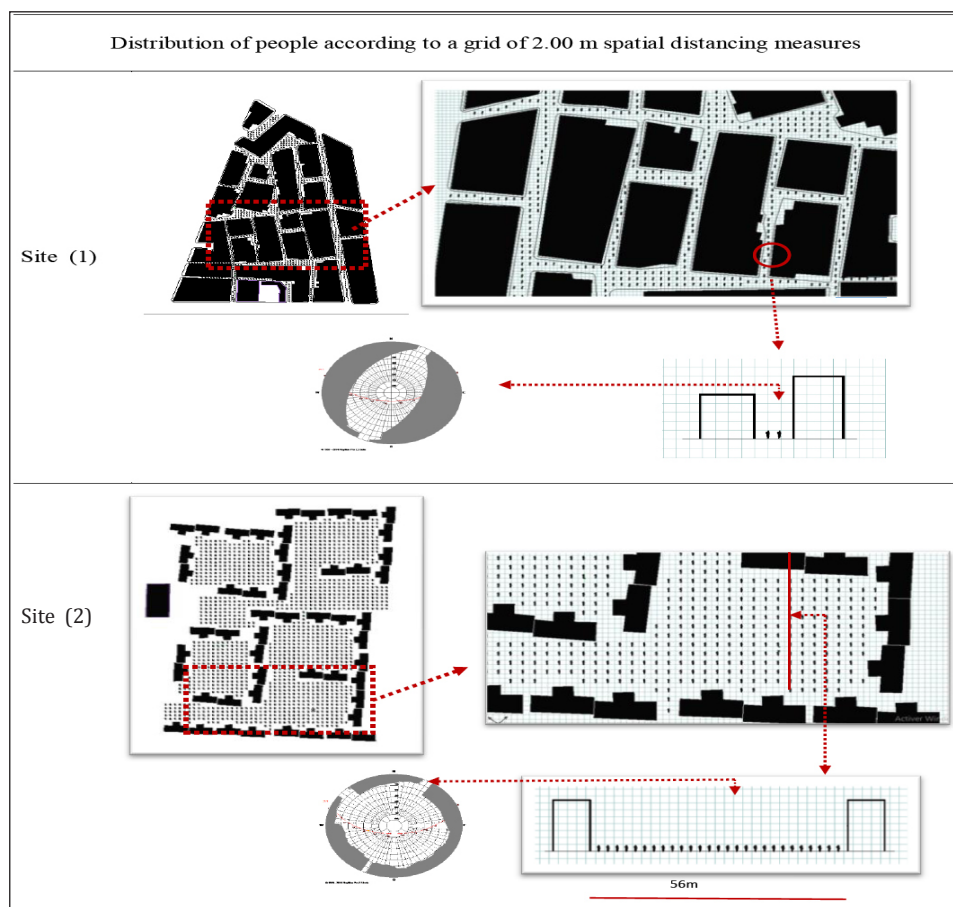
These results confirm that the density of the fabric has a direct impact on the SVF and the H/L ratio, which affect the spread of the COVID 19 virus; we can deduce that this allows better solar exposure, psychological relief and more appropriate air ventilation [31, 32].

In the sparse urban fabric (2), built area (17%), where the free surface is estimated at 54633.92 m<sup>2</sup>, and if the distance from each individual is 2.00 m, and in order to reduce the rate of cross infection, we will have a total number of 3414 individuals at once. In percentage; 136.56% at the same time in this space, when really the number of individuals in the whole city is estimated at 2500 individuals, so we deduce that the cross-infection rate to Covid 19 is practically nil.



On the contrary, in the urban fabric (1) dense, built area (67%), where the free surface is estimated at 24064 m<sup>2</sup>, and with the same distance, we will have a number of 1504 individuals. In percentage; 57.66% at the same time in this space while the total number of the population in this fabric is estimated at 2608 inhabitants, we deduce that the rate of cross-infection with Covid 19 is high during the year 2020. Table 6 and Table 07.

**Table 6.** Distribution of people according to a grid of 2m spatial distancing measures in the two urban configurations and their occupation behavior.



**Table 7.** Assessment of the two urban configurations' spatial factors

Settings	Site n° (1)	Site No. (2)
Urban density CES	67 %	17 %
The unbuilt surface	24064 m <sup>2</sup>	54633.92 m <sup>2</sup>
Space dimensions (average H/L ratio)	1.51	0.27
Sky View Factor (SVF)	0.40	0.80
Population number in both neighborhoods	2608 inhabitants	2500 inhabitants
Maximum number of users ( 2.00 m) distanc	1504 people, in percentage 58%	3414 people, in percentage 137%

Spatial distancing could transform urban space in order to preserve the well-being of our cities, while limiting the spread of the pandemic. The minimum distances we should observe to avoid contamination are estimated at 1.80m to 2.00m, [12,24–26] In our case, we have adopted a distribution of people, according to a grid of spatial distance measurements determined as 2.00 m, to avoid contamination of Covid-19.

Finally, we can conclude that the lower the density of the building, the morphological and geometric indicators (SVF tending towards the value 1 and H/L tending towards 0), the healthier these spaces are. Moreover, vice versa, they will become contagious, allowing the spread of the virus. [11, 33–35] .

## Comparison between the Impacts of Micro-Climatic Parameters on the Spread of the Pandemic in the Two Urban Configurations

In the following, we present the comparison of microclimatic variables between site (1) and site (2), to highlight the impact of microclimatic parameters of urban spaces on the pandemic proliferations of COVID-19.

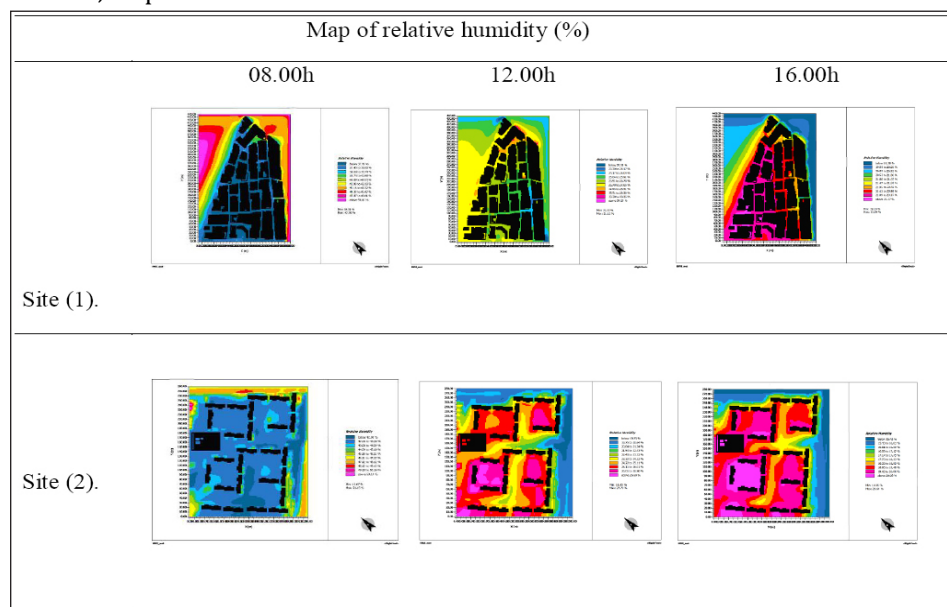
The simulation allows us to measure the evolution of the following microclimatic parameters: air temperature (°C), relative humidity (%), direct solar radiation (KWh/m<sup>2</sup>) and air speed (m/s). We carried out this analysis for the summer period in order to access the microclimatic performance of each urban space during the pandemic, according to three schedules, as follows: in the morning at 8:00 a.m., midday at 12:00 p.m. and in the evening at 4:00 p.m.

### Impact of Relative Humidity on the Spread of the Pandemic in the Two Urban Configurations

For the spatial distribution of the relative humidity of the two sites (1) and (2), we present them in the maps below, obtained from the results of the relative humidity simulation. There is a decrease in the values of this, as time passes on the site (1), it decreases from 37.45% at 08:00 to 25.91% to end at 23.37% at 16:00. It is the same a site (2), but the variation of this decrease is more accelerated. The values of relative humidity are 43.50%, 25.88% and 19.00% respectively at 08:00, 12:00, and 4:00 p.m. certainly these amounts are due to the great opening of spaces in that case.

According to the standards, a higher percentage of relative humidity increases the spread of the virus and that it decreases in the case of low percentages. It is high when RH > 70%, medium when it is between 50% to 70%, and low when HR < 50% [12,34–36]. In our case, and despite the variations observed, they remain in both cases below 50%, consequently and depending on the relative humidity, the spread of the pandemic remains low in the two urban configurations. Table 8.

**Table 8.** Comparison between relative humidity % of the two urban configurations: site (1) and site (2) on the spread of the pandemic at 8 a.m., 12 p.m. and 4



### Impact of Air Temperature on the Spread of the Pandemic in the Two Urban Configurations

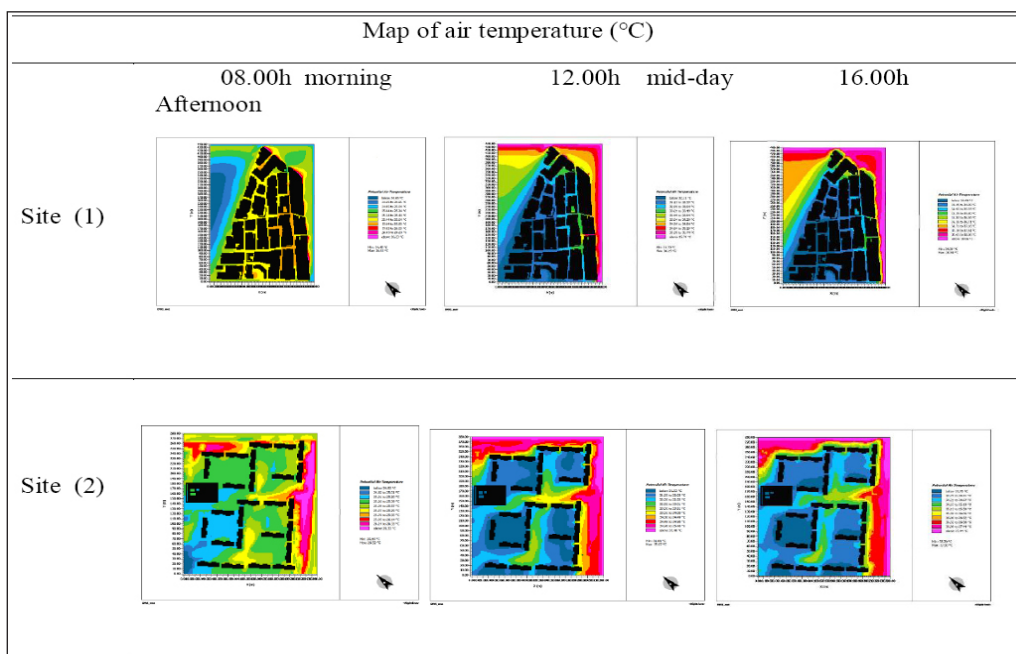
The spatial distribution of the temperatures of the two sites (1) and (2) is presented in the maps, below, obtained from the results of the simulation; these illustrate the different values according to the morphology of the space.

Overall, we can deduce that the temperatures rise in both cases, as time passes and this, until 4:00 p.m., with higher values of site (2) compared to site (1), obviously this is due to the greater shade of the site (1) and to direct exposure to solar radiation from the large open spaces of the site (2).

According to the results of some research in this theme, these state that high temperatures decrease the spread of the virus than low temperatures. [12, 21, 34, 35]. Consequently, and during the morning, the two sites present, in relation to the climatic parameter air temperatures, identical virus propagation conditions given their low temperatures, and as

time passes and with increasing temperature, this propagation ability decreases with an advantage of the site (2), since its temperature is the highest. Table 9.

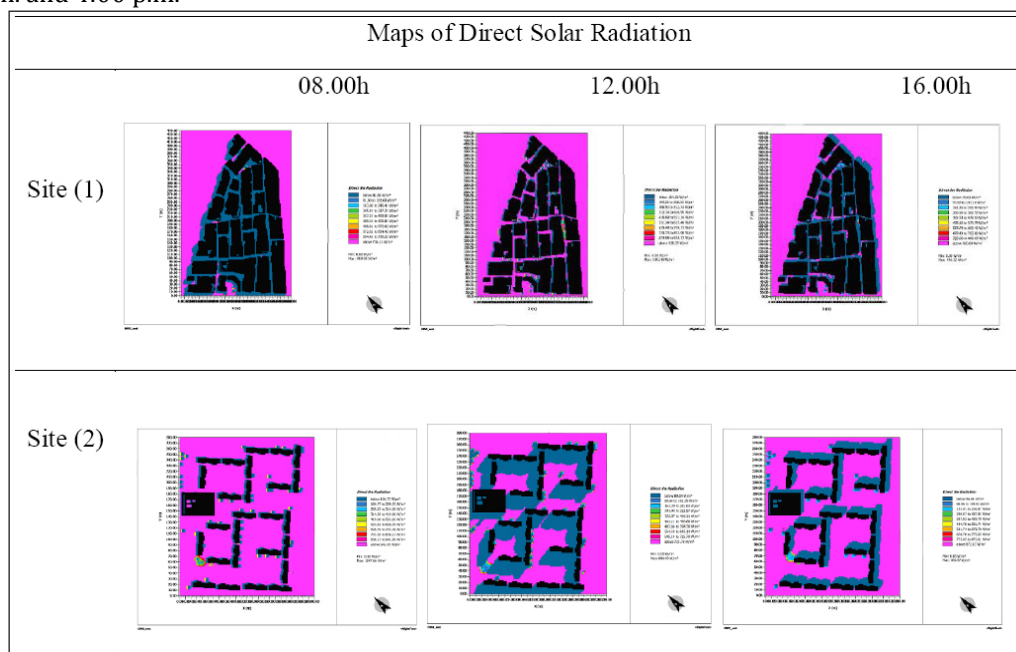
**Table 9.** The comparison of air temperatures between the two urban configurations of the pandemic spread through the day at 08h00, 12h00 and 16h00.



### Impact of Direct Solar Radiation on the Spread of the Pandemic in the Two Urban Configurations

The spatial distribution of direct radiation from the two Sites number (1) and (2) is presented in the maps below, obtained from the simulation results. High solar radiation values are shown in purple color, while lower values are shown in blue color. The results show that Kemouni (site1) records reduced solar radiation values compared to the 500-dwelling district site (2) with an average deviation  $\Delta T = 5.4$  (KWh/m<sup>2</sup>) in favor of a site (2). This is primarily caused by the relation between H/L and SVF. Table 10.

**Table 10.** Maps of spatial distribution of the difference in direct solar radiation in the two urban configurations; at 8:00 a.m., 12:00 p.m. and 4:00 p.m.



The values of direct solar radiation increase with the increase in the values of the SVF and the decrease in the values of the H/L ratio; this is remarkable in the two subdivisions [43] .

Table 11, below, illustrates three solar climate zones with different impacts on public health. These areas improve the immune system by allowing photosynthesis of vitamin D or cause skin burns [16,17,20,27–30].

**Table11.** The evaluation of solar radiation (KWh/m2) in relation to surfaces (m2) for the two urban configurations.

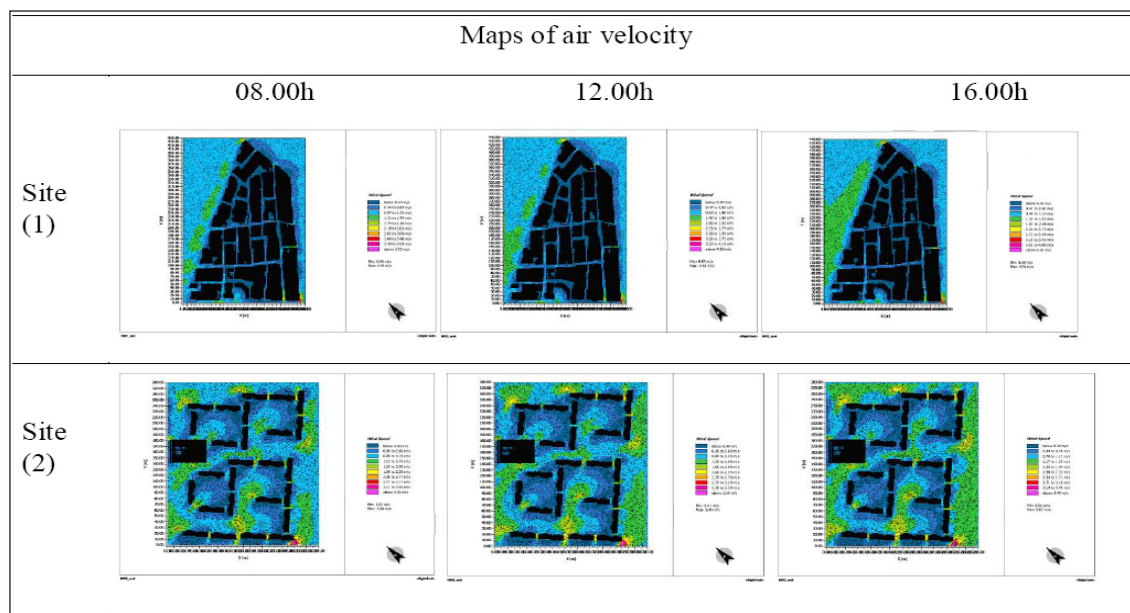
Site	Free area (m 2)	Scale (KWh/m2)	(m2)
Site (1)	24064.00	a) Low < 4,5 KWh/m2 b) Moderate 4.5–5.5 kWh/m2 c) High> 5,5 KWh/m2	a) 19831.00 b) 4234.00 c) 00000.00
Site (2)	54633.92		a) 22853.72 b) 32380.00 c) 00000 .00

### Impact of Airspeed on the Pandemic Spread in the Two Urban Configurations

The values of the airspeed of site n° (2) are higher than the airspeed of site n° (1). This is certainly due to the morphology of the alleys, where they are minimal due to their narrowness. The minimum values in blue color persist throughout the day at this site. Unlike site n° (2) where the variety of colors testifies to the variation in airspeed between the different outdoor spaces, and even between the morning, afternoon and evening. The blue concentration corresponds to the lowest speeds. The decrease in the H/L ratio between the layouts of the two sites makes it possible to assess an average increase in air speed of 1.75 m/s at the profile of Site (2), at this site, the phenomenon is mainly due to the same height of the buildings, but a significant widening of the tracks. [15, 43] .These differences between the airspeeds are mainly due to the following elements, which are not taken into account by the directional opening:

- Density effect: Site (1) has a strong built density. The building prospects are indeed quite large while those on the streets are very low. This density effect will therefore reduce the permeability of the streets to the wind. Beyond this face, the wind only penetrates the streets through the peripheral limits of the district. Table 12.

**Table 12.** Maps of spatial distribution of air speed in site (1) and site (2) for the day at 08h00a.m., 12h00 p.m., and 04h00 p.m.



In recent research, high ventilation rates have been stated to contribute to droplet scattering, while poorly ventilated areas contribute to droplet accumulation over time. Therefore, spaces with sufficient ventilation have lower risks of



infection (Qian in 2010). This means that areas with sufficient airspeed capacity would dilute infectious droplets and reduce the risk of transmission [43] Dilute the infectious droplets allows the dispersion of the droplets and prevents their accumulation, therefore, it decreases the infection and improves mental health.[5, 12, 14, 25, 31–33]. In our two cases, no exterior surface is subjected to an airspeed greater than 5 m/s, while the site (2) has an estimated surface of 20616m<sup>2</sup> subjected to an airspeed of between 2.5m/s and 5m/s. Compared to this airspeed interval, the external surface of the site (1) subject to it is only about 751m<sup>2</sup>. The rest of the exterior surfaces at the two sites are subject to airspeed of less than 2.5m/s. Table 13

**Table 13.** Evaluation of surfaces subject to different wind speeds for the two urban configurations.

Site	Unbuilt area (m <sup>2</sup> )	Air velocity m/s	(m <sup>2</sup> )
Site (1)	24064.00	* <2.5m/s	23313.08
		* 2.5-5m/s	750.92
		* >5m/s	000.00
Site (2)	54633.92	* <2.5m/s	34 017.41
		* 2.5-5m/s	20616.51
		* >5m/s	000.00

The results obtained in this article are summarized in tables 10, 11, 12 and 13 illustrating the areas (m<sup>2</sup>) of adequate solar radiation (KWh/m<sup>2</sup>) and the values of adequate natural ventilation (m/s)

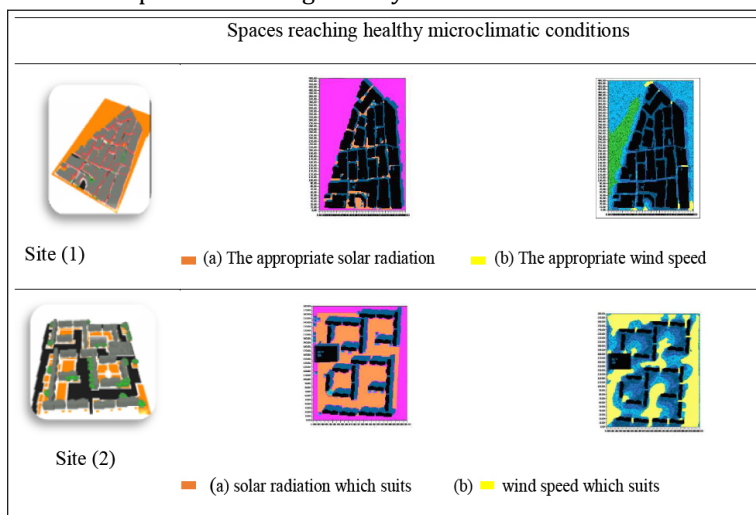
Table 14 presents the zones exhibiting healthy micro-climatic conditions through an evaluation of the optimal values of natural ventilation and solar radiation calculated for the two urban configurations. The areas were calculated following the framework for the quantitative assessment of morpho-climatic parameters during the pandemic, illustrated in Table1.

**Table 14.** The zones exhibiting healthy microclimatic conditions for the two urban configurations.

site	Unbuilt area (m <sup>2</sup> )	healthy surface (m <sup>2</sup> )	percentage %
Site (1)	24064.00	750.92	03.12%
Site (2)	54633.92	20616.51	37.73%

Site (1) records very small areas with healthy micro-climatic performance. It displayed an adequate area equal to 750.92 m<sup>2</sup>, which represents 03.12% of its total area. It is reported that the site (2) registers a consequent surface with acceptable micro-climatic behavior, reaching 20616.51 m<sup>2</sup>, which represents approximately 37.73%, of its total free surface. In both cases, the results are based on their optimal micro-climatic performance in terms of solar radiation and air movement. As shown in Table 15

**Table 15.** Graphic representation of spaces achieving healthy microclimatic conditions in the two urban configurations.



After studying two of the main open spaces of the urban fabric of Batna city, using measurements and numerical simulations, the search results recommended that the site (2) should be used for public use during pandemics. It gets a score of 8/9 compared to the site (1) which gets 1/9. According to the novelty of the subject, this evaluation remains theoretical as long as it is validated by modeling, simulations and on-site measurements. The previous results are summarized in table 16.

**Table 16.** The morpho-climatic balance of the two urban configurations.

Settings	Site No. (1)	Site No. (2)	Optimum
Urban density CES	67%	17%	Site (2)
Healthy space dimensions (H/L ratio)	1.51	0.27	Site (2)
Sky View Factor (SVF)	0.40	0.80	Site (2)
Maximum number of users (2.00 m distance)	1504 people, equivalent to 58%	3414 people, Equivalence to 137%	Site (2)
The effective solar exposure surface (m <sup>2</sup> ).	17.60%	59.27%	Site (2)
The effective natural ventilation area (m <sup>2</sup> ).	03.12%	37.73%	Site (2)
the average percentage of relative humidity	28.91%	29.46%	Site (2)
Average air temperature (°C)	30.91	30.55	Site (1)
Air quality index (AQI)	57%	57%	-
Percentage surface area of spaces reaching healthy microclimatic conditions	03.12%	37.73%	Site (2)
	03.12%	37.73%	Site (2)
Total score			8/9 Site (2)

## CONCLUSION

The importance of this study came from the importance of reviewing urban actions in the light of the Covid-19 pandemic and the new social life, and responding to the imperative demand requiring the involvement of planners and urban planners in pandemic disaster management strategies.

From this experiment, we retain that the urban density has a considerable effect on the morphological indicators, in particular the two essential parameters; namely the SVF and the H/L ratio. They impact the maximum number of users with consideration of the previously defined distance, at 2.00 m in our case, and ratify a new typology of design, according to public safety measures to produce compliant urban spaces. The outdoor urban spaces were characterized, during the simulations, by the sky view factor and the H/L ratio, which affect the microclimatic variations, where we noticed strong correlations between the two morphological parameters; direct solar radiation and airspeed, and the spread of the pandemic. The results obtained show that an urban area with low SVF promotes pandemic proliferations of COVID-19 during the day, unlike an area with high SVF. This is because; the lower the density of the building, the morphological and geometric indicators are transformed so that the SVF factor tends towards the value 1 and the H/L ratio tends towards 0, which allows these spaces to have good climatic performances, becoming healthier. Conversely, they allow contagion and facilitate the spread of the virus, paradoxically by ensuring thermal comfort. Social distancing has had a great positive impact on reducing the risk of infection, but we can conclude that the search for a new vision of designing quality public spaces, healthy and satisfying the new needs of the inhabitants, is the solution to major health crisis. The assessment prioritized and categorized spaces with adequate micro-climatic behavior to be engaged in public life during periods of confinement. It turned out that the loose fabric like site no (2) is the ideal model, providing the optimal urban and environmental performance during pandemics, without any intervention to fight infection. It therefore appears that a new concept (strategy) of urban spatial design should be introduced as freely as possible and independently of other pandemic mitigation interventions.

**Funding:** This research received no external funding

**Data Availability Statement:** Interview with the head of the covid-19 service at the level of the health directorate of Batna Wilaya.

**Acknowledgments:** We acknowledge the support of the laboratory Lacomofa by the materials used for in situ measures and the software program used in this work

**Conflicts of Interest:** The authors declare no conflict of interest.

## REFERENCE

1. Sharifi, A.; Khavarian-Garmsir, A.R. The COVID-19 Pandemic: Impacts on Cities and Major Lessons for Urban Planning, Design, and Management. *Sci Total Environ* 2020, 749, 142391, doi:10.1016/j.scitotenv.2020.142391.
2. Samuelsson, K.; Barthel, S.; Colding, J.; Macassa, G.; Giusti, M. *Urban Nature as a Source of Resilience during Social Distancing amidst the Coronavirus Pandemic*; 2020;
3. Neiderud, C.-J. How Urbanization Affects the Epidemiology of Emerging Infectious Diseases. *Infect Ecol Epidemiol* 2015, 5, 10.3402/iee.v5.27060, doi:10.3402/iee.v5.27060.
4. World Health Organization *Rational Use of Personal Protective Equipment for Coronavirus Disease (COVID-19): Interim Guidance*, 27 February 2020; World Health Organization, 2020;
5. Stevens, N.J.; Tavares, S.G.; Salmon, P.M. The Adaptive Capacity of Public Space under COVID-19: Exploring Urban Design Interventions through a Sociotechnical Systems Approach. *Human Factors and Ergonomics in Manufacturing & Service Industries* 2021, 31, 333–348, doi:10.1002/hfm.20906.
6. Liu, Z. Sustainable Tourism Development: A Critique. **2003**, doi:10.1080/09669580308667216.
7. Sun, C.; Zhai, Z. The Efficacy of Social Distance and Ventilation Effectiveness in Preventing COVID-19 Transmission. *Sustain Cities Soc* 2020, 62, 102390, doi:10.1016/j.scs.2020.102390.
8. Mesa Vieira, C.; Franco, O.H.; Gómez Restrepo, C.; Abel, T. COVID-19: The Forgotten Priorities of the Pandemic. *Maturitas* **2020**, 136, 38–41, doi:10.1016/j.maturitas.2020.04.004.
9. Ali, Q.; Raza, A.; Saghir, S.; Khan, M.T.I. Impact of Wind Speed and Air Pollution on COVID-19 Transmission in Pakistan. *Int. J. Environ. Sci. Technol.* 2021, 18, 1287–1298, doi:10.1007/s13762-021-03219-z.
10. Franch-Pardo, I.; Napoletano, B.M.; Rosete-Verges, F.; Billa, L. Spatial Analysis and GIS in the Study of COVID-19. A Review. *Science of The Total Environment* 2020, 739, 140033, doi:10.1016/j.scitotenv.2020.140033.
11. Prapamontol, T.; Norbäck, D.; Thongjan, N.; Suwannarin, N.; Somsunun, K.; Ponsawansong, P.; Radarit, K.; Kawichai, S.; Naksen, W. Asthma and Rhinitis in Wet and Dry Season among Students in Upper Northern Thailand: The Role of Building Dampness and Household Air Pollution. *International Journal of Environmental Health Research* 2022, 0, 1–13, doi:10.1080/09603123.2022.2047902.
12. Franch-Pardo, I.; Napoletano, B.; Rosete, F.; Billa, L. Spatial Analysis and GIS in the Study of COVID-19. A Review. *Science of The Total Environment* 2020, 739, 140033, doi:10.1016/j.scitotenv.2020.140033.
13. Rendana, M. Impact of the Wind Conditions on COVID-19 Pandemic: A New Insight for Direction of the Spread of the Virus. *Urban Climate* 2020, 34, 100680, doi:10.1016/j.uclim.2020.100680.
14. Leng, L.; Xu, S.; Liu, R.; Yu, T.; Zhuo, X.; Leng, S.; Xiong, Q.; Huang, H. Nitrogen Containing Functional Groups of Biochar: An Overview. *Bioresource Technology* 2020, 298, 122286, doi:10.1016/j.biortech.2019.122286.
15. Sun, C.; Zhai, Z. The Efficacy of Social Distance and Ventilation Effectiveness in Preventing COVID-19 Transmission. *Sustain Cities Soc* 2020, 62, 102390, doi:10.1016/j.scs.2020.102390.
16. Sleijffers, A.; Garssen, J.; Vos, J.G.; van Loveren, H. Ultraviolet Light and Resistance to Infectious Diseases. *Journal of Immunotoxicology* 2004, 1, 3–14, doi:10.1080/15476910490438333.
17. Juzeniene, A.; Ma, L.-W.; Kwitniewski, M.; Polev, G.A.; Lagunova, Z.; Dahlback, A.; Moan, J. The Seasonality of Pandemic and Non-Pandemic Influenzas: The Roles of Solar Radiation and Vitamin D. *International Journal of Infectious Diseases* 2010, 14, e1099–e1105, doi:10.1016/j.ijid.2010.09.002.
18. Bassil, D.; Rahme, M.; Hoteit, M.; Fuleihan, G.E.-H. Hypovitaminosis D in the Middle East and North Africa. *Dermato-Endocrinology* 2013, 5, 274–298, doi:10.4161/derm.25111.

19. Normal Vitamin D Levels: Ranges by Age Available online: <https://www.medicalnewstoday.com/articles/normal-vitamin-d-levels> (accessed on 6 June 2022).
20. Flies, E.J.; Mavoa, S.; Zosky, G.R.; Mantzioris, E.; Williams, C.; Eri, R.; Brook, B.W.; Buettel, J.C. Urban-Associated Diseases: Candidate Diseases, Environmental Risk Factors, and a Path Forward. *Environment International* 2019, 133, 105187, doi:10.1016/j.envint.2019.105187.
21. Wang, J.; Tang, K.; Feng, K.; Lv, W. *High Temperature and High Humidity Reduce the Transmission of COVID-19*; 2020;
22. Urban Landscapes and Identity | IntechOpen Available online: <https://www.intechopen.com/chapters/45403> (accessed on 7 June 2022).
23. Garden, A. de, Sebastian "Urban Space" by ROB KRIER | Architect & Sculptor Available online: <http://robkrier.de> (accessed on 7 June 2022).
24. World Health Organization *Rational Use of Personal Protective Equipment for Coronavirus Disease (COVID-19): Interim Guidance, 27 February 2020*; World Health Organization, 2020;
25. Mesa Vieira, C.; Franco, O.H.; Gómez Restrepo, C.; Abel, T. COVID-19: The Forgotten Priorities of the Pandemic. *Maturitas* 2020, 136, 38–41, doi:10.1016/j.maturitas.2020.04.004.
26. de Kadt, J.; Götz, G.; Hamann, C.; Maree, G.; Parker, A. *Mapping Vulnerability to COVID-19 in Gauteng*; Map of the Month; Gauteng City-Region Observatory, 2020;
27. Bassil, D.; Rahme, M.; Hoteit, M.; Fuleihan, G.E.-H. Hypovitaminosis D in the Middle East and North Africa: Prevalence, Risk Factors and Impact on Outcomes. *Dermatoendocrinol* 2013, 5, 274–298, doi:10.4161/derm.25111.
28. Swaminathan, A.; Harrison, S.L.; Ketheesan, N.; van den Boogaard, C.H.A.; Dear, K.; Allen, M.; Hart, P.H.; Cook, M.; Lucas, R.M. Exposure to Solar UVR Suppresses Cell-Mediated Immunization Responses in Humans: The Australian Ultraviolet Radiation and Immunity Study. *Journal of Investigative Dermatology* 2019, 139, 1545-1553.e6, doi:10.1016/j.jid.2018.12.025.
29. Junaid, K.; Rehman, A. Impact of Vitamin D on Infectious Disease-Tuberculosis-a Review. *Clinical Nutrition Experimental* 2019, 25, 1–10, doi:10.1016/j.clnex.2019.02.003.
30. New World Bank Tool Helps Map Solar Potential Available online: <https://www.worldbank.org/en/news/press-release/2017/01/17/new-world-bank-tool-helps-map-solar-potential> (accessed on 8 June 2022).
31. Morawska, L.; Cao, J. Airborne Transmission of SARS-CoV-2: The World Should Face the Reality. *Environment International* 2020, 139, 105730, doi:10.1016/j.envint.2020.105730.
32. Shooshtarian, S.; Rajagopalan, P. Perception of Wind in Open Spaces. *Climate* 2019, 7, 106, doi:10.3390/cli7090106.
33. Gao, G.; McMahon, C.; Chen, J.; Rong, Y.S. A Powerful Method Combining Homologous Recombination and Site-Specific Recombination for Targeted Mutagenesis in *Drosophila*. *Proc. Natl. Acad. Sci. U.S.A.* 2008, 105, 13999–14004, doi:10.1073/pnas.0805843105.
34. Lowen, A.C.; Steel, J.; Mubareka, S.; Palese, P. High Temperature (30°C) Blocks Aerosol but Not Contact Transmission of Influenza Virus. *Journal of Virology* 2008, 82, 5650–5652, doi:10.1128/JVI.00325-08.
35. Tan, L.H.; Laird, A.R.; Li, K.; Fox, P.T. Neuroanatomical Correlates of Phonological Processing of Chinese Characters and Alphabetic Words: A Meta-Analysis. *Human Brain Mapping* 2005, 25, 83–91, doi:10.1002/hbm.20134.
36. Abd Elrahman, A.S. The Fifth-Place Metamorphosis: The Impact of the Outbreak of COVID-19 on Typologies of Places in Post-Pandemic Cairo. *Archnet-IJAR: International Journal of Architectural Research* 2020, 15, 113–130, doi:10.1108/ARCH-05-2020-0095.
37. Bruse, M.; Fleer, H. Simulating Surface-Plant-Air Interactions inside Urban Environments with a Three Dimensional Numerical Model. *Environmental Modelling & Software* 1998, 13, 373–384, doi:10.1016/S1364-8152(98)00042-5.



38. Laffta, S.; Alrawi, A. Planning of Sustainable Industrial Zones and Means of Achieving Them in Iraq. *KnE Engineering* 2018, 3, 259, doi:10.18502/keg.v3i4.2173.
39. A Multi-Modal Hierarchical Recurrent Neural Network for Depression Detection | Proceedings of the 9th International on Audio/Visual Emotion Challenge and Workshop Available online: <https://dl.acm.org/doi/abs/10.1145/3347320.3357696> (accessed on 7 June 2022).
40. Djaghrouri, D. Fluctuation Des Ambiances Thermiques Extérieures Sous l'effet Du Végétal Dans Les Zones Arides. « Cas d'une Placette à Biskra Ville ». doctoral, Université Mohamed Khider – Biskra, 2021.
41. Fouad, A.O. Morphologie urbaine et confort thermique dans les espaces publics : étude comparative entre trois tissus urbains de la ville de Québec. 2007.
42. Colombert, M. Contribution à l'analyse de la prise en compte du climat urbain dans les différents moyens d'intervention sur la ville. phdthesis, Université Paris-Est, 2008.
43. Elsayed, D.S.I. The Microclimatic Impacts of Urban Spaces on the Behaviour of Pandemics between Propagation and Containment: Case Study Historic Cairo. *Urban Climate* 2021, 36, 100773, doi:10.1016/j.uclim.2021.100773.
44. Samira, B.; Bouchahm, Y. Numerical Simulation of Effect of Urban Geometry Layouts on the Wind in Outdoor Spaces under Mediterranean Climate. 2017, 6.

**Citation:** DJAGHROURI Djamila, ZERAIB Salah, et al. *The Impacts of Morpho-Climatic Parameters on Pandemic Proliferations of Covid-19 between Expansion and Confinement in Semi-Arid Areas: Case of Batna City (Algeria)*. *Int J Innov Stud Sociol Humanities*. 2022;7(7):69-85. DOI: <https://doi.org/10.20431/2456-4931.070707>.

**Copyright:** © 2022 The Author(s). This open access article is distributed under a Creative Commons Attribution (CC-BY) 4.0 license